

## Supplementary Section

Several studies indicated the impact of different parameters on the relative dispersion of the cloud droplets ( $\epsilon$ ), including aerosol loading, dynamic and microphysical parameters, as well as altitude above cloud base (see Sect. 1). In this paper we observed that in warm Cu clouds none of the above mentioned parameters showed significant trends with the magnitude of  $\epsilon$ . The variance of  $\epsilon$ , however, was shown to be smaller with increasing liquid water content (LWC) and cloud droplet concentrations ( $N_c$ ).

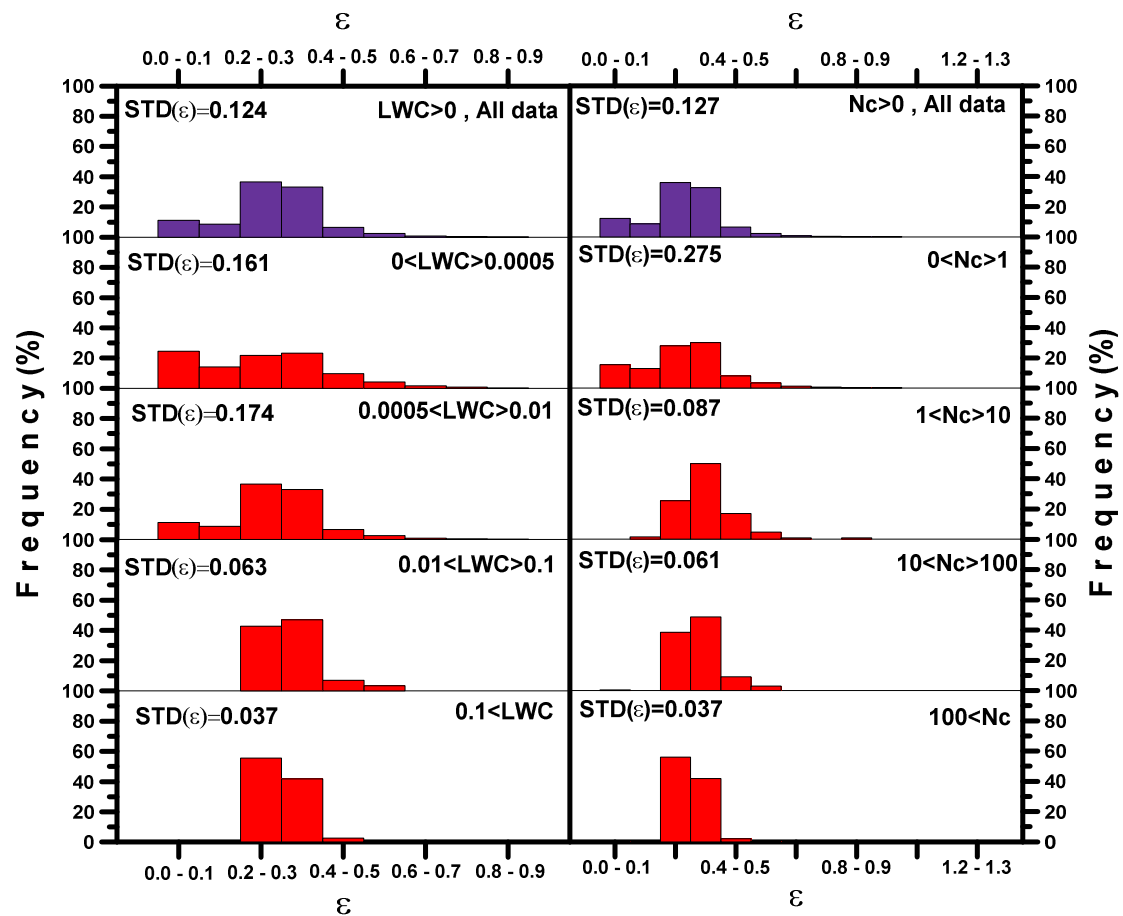
Figure S1 presents histograms of  $\epsilon$  for different LWC and  $N_c$ . The histograms are based on data collected during four of the flights, excluding the data which was collected during TRK3, due to measurements limitation on that day (see Section 3). Figures S1 indicates that the variance of  $\epsilon$  tends to decrease for increasing values of  $N_c$  and LWC. Figure S2 presents separate histograms of  $\epsilon$  for each flight, excluding data associated with  $N_c < 10 \text{ cm}^{-3}$ . This figure demonstrates that  $\epsilon$  variance decreases for flights associated with higher aerosol loading, which may be related to increasing  $N_c$  and/or LWC, and extension of the relative duration of the mature stage with increasing aerosol loading as suggested by the second indirect effect (Albrecht et al., 1989).

Figure 3S presents  $\epsilon$  histograms for different segments along the vertical depth of the cloud. This graph indicates that the variance of  $\epsilon$  tends to be lower within or near cloud base, than higher in the cloud. This difference can be associated with formation of new droplets or the detection of droplets that are initially smaller than the lower threshold of the instruments. Such effect could explain the widening of the distribution, thus negating the narrowing trends due to condensation, leading to more confine values of  $\epsilon$  near cloud base. Fig. 3S further suggests that  $\epsilon$  doesn't show any

significant trend with increasing height, above cloud base.

26

27



28

Figure S1. Histograms of  $\epsilon$  for different LWC and  $N_c$ . This figure presents LWC (in gr/Kg) and  $N_c$  ( $\#/cm^3$ ) ranges, as indicated individually for each panel. The upper panels (labeled as “ALL data”) are based on all measured data during all flights. All other histograms use only data range, which is specified individually in each panel. Data collected during flight TRK3 was not used for any of the histograms. The standard deviation for each histogram is specified by “STD” for each histogram.

29

30

31

32

33

34

35

36

37

38

39

40

41

42

43

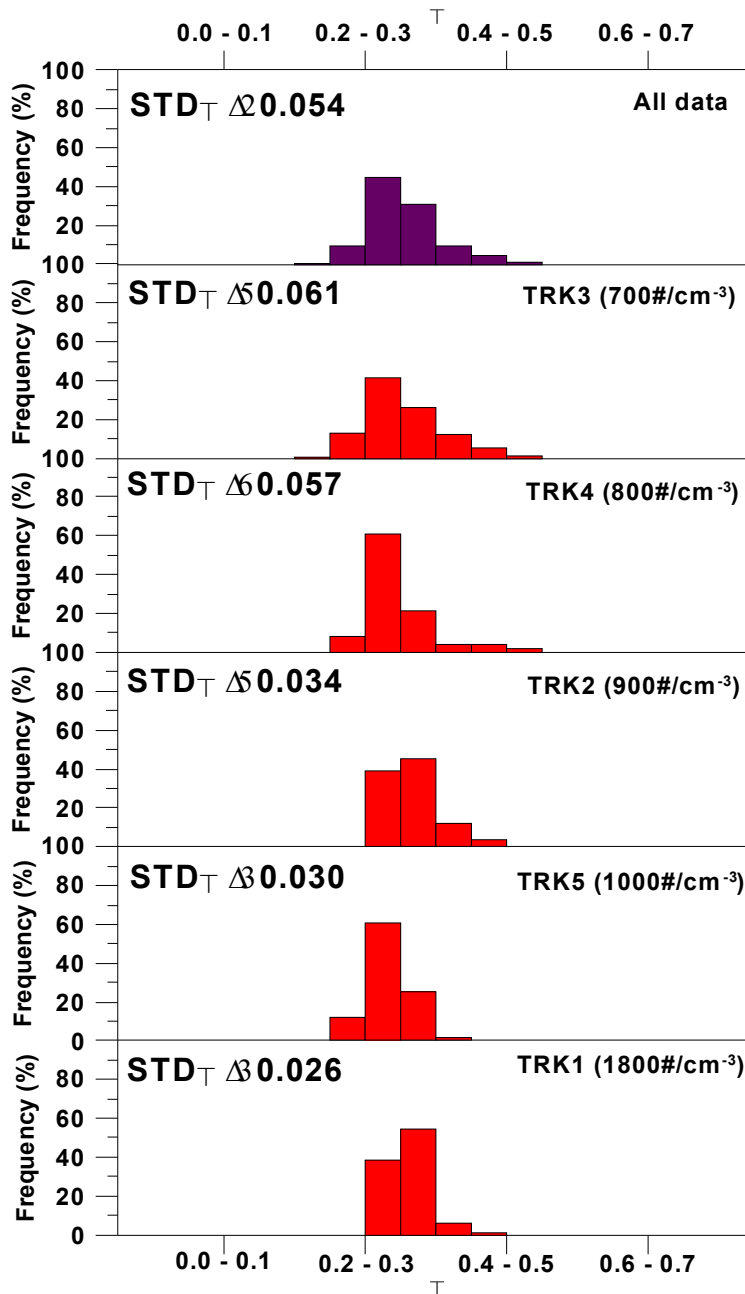


Figure S2. Histograms of  $\epsilon$  for different aerosol loadings. This figure presents  $\epsilon$  histograms for each flight, in order to test the impact of aerosol loading on  $\epsilon$  dispersion. The average aerosol loading for each flight (calculated at cloud base height out of the cloud) is presented for each flight. All histograms are based only on measured data associated with  $N_c > 10$ . The histogram in the upper panel is based on data collected during all flights.

44  
45  
46  
47  
48  
49  
50  
51  
52  
53  
54  
55  
56

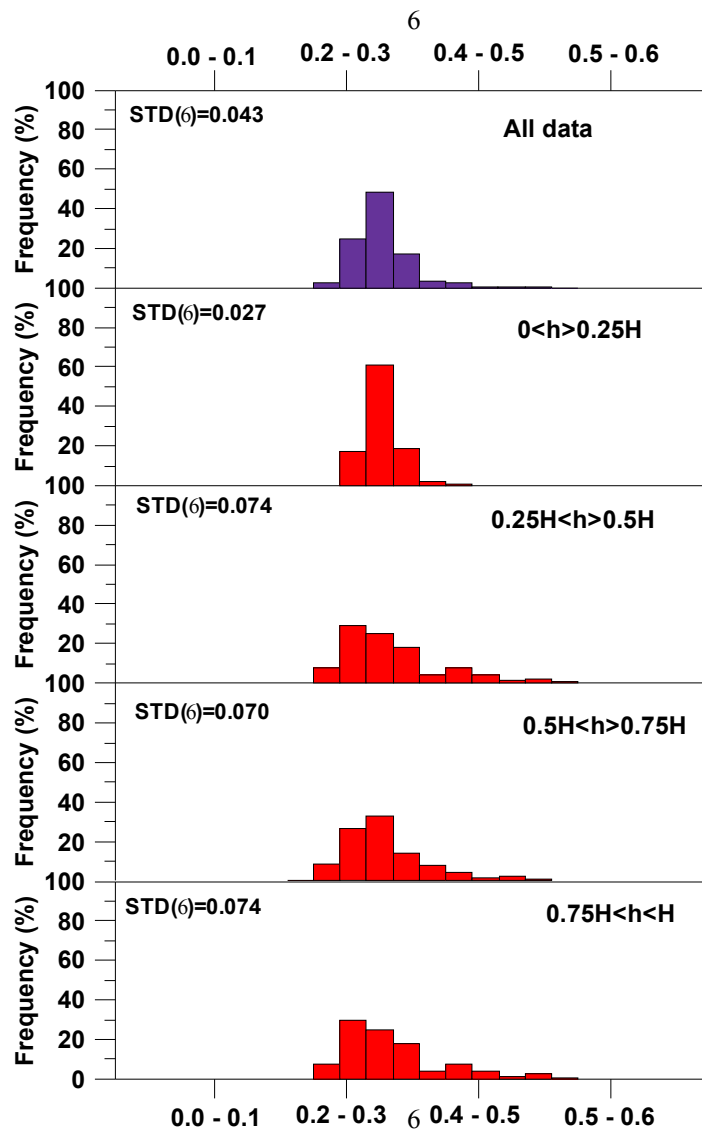


Figure S3. Histogram of  $\epsilon$  for different height ranges above cloud base (indicated individually for each histogram by “h” range of the total cloud depth, “H”). All histograms are based only on measured data associated with  $N_c > 10$ . The upper panel is based on data collected during all flights. Data collected during flight TRK3 was not used for any of the histograms.

57  
58  
59  
60  
61  
62  
63  
64  
65  
66